Two Comparison-Alternative High Temperature PCB-Embedded Transformer Designs for a 2 W Gate Driver Power Supply

Bingyao Sun, Rolando Burgos, Dushan Boroyevich, Remi Perrin, Cyril Buttay, Bruno Allard, Nicolas Quentin, Marwan Ali

Two Comparison-Alternative High Temperature PCB-Embedded Transformer Designs for a 2 W Gate Driver Power Supply

Bingyao Sun, Rolando Burgos, Dushan Boroyevich
Center for Power Electronics Systems
The Department of Electrical and Computer Engineering
Virginia Tech
Blacksburg, USA
bingyao@vt.edu

Remi Perrin, Cyril Buttay, Bruno Allard, Nicolas Quentin, Marwan Ali
Ampere lab
INSA Lyon, Univ. Lyon
Lyon, France
remi.perrin@insa-lyon.fr

***Abstract*— With fast power semiconductor devices based on GaN and SiC becoming more common, there is a need for improved driving circuits. Transformers with smaller inter-winding capacitance in the isolated gate drive power supply helps in reducing the conducted EMI emission from the power converter to auxiliary sources. This paper presents a transformer with a small volume, a low power loss and a small inter-capacitance in a gate drive power supply to fast switching devices, such as GaN HEMT and SiC MOSFET. The transformer core is embedded into PCB to increase the integration density. Two different transformer designs, the coplanar-winding PCB embedded transformer and the toroidal PCB embedded transformer, are presented and compared. The former has a 0.8 pF inter-capacitance and the latter has 85% efficiency with 73 W/in^3 power density. Both designs are dedicated to a 2 W gate drive power supply for wide-band-gap device, which can operate at 200℃ ambient temperature.**

Keywords—GaN, PCB-embedded transformer, high integration converter, inter-capacitance, high temperature

I. INTRODUCTION

Fast-switching power devices, such as GaN HEMT and SiC MOSFET, have enabled converters to achieve higher switching frequency, higher efficiency, and higher power density. The fast switching transient results in low switching losses though it tends to aggravate EMI. To enhance the EMI immunity of the whole system, the transformer in the isolated gate drive power supply should have a small inter-winding capacitance. High power density and high efficiency are also another important factors in terms of converter design.

The integration of passive components is a key enabler for high-power-density power supply [1] [2]. The low-cost printed circuit board (PCB) is the most widely used substrate material in electronic applications [3] [4]. The PCB material selected as the substrate material to integrate a high power-density converter is mainly because of its capability for high-volume production using standard lamination process.

This study details a comparative work of two ways to embed magnetic into PCB. Two different transformer structures are both optimized to have a PCB thickness as thin as possible. This point is motivated to limit the delamination issue due to a too high PCB stack [5] and to have a converter size as small as possible. The magnetic material of the both designs is carefully selected, guaranteeing a lower transformer loss [6] and holding the mechanical pressure during the PCB lamination process. The high temperature PCB material R-1515, is selected and suggests the potential to use the transformer in high temperature application, holding 200℃. This work interest is multiple. First the resonant active clamp flyback topology is selected according to the high-temperature low-power power supply requirement. The two corresponding PCB embedded transformer designs dedicated to this topology is processed with optimizations. The transformer performances between the two PCB-embedded designs are compared afterwards with the high frequency converter.

This work is sponsored by SAFRAN, FRANCE.

II. TOPOLOGY: ACTIVE-CLAMP FLYBACK

The gate drive power supply is dedicated to support one phase-leg of 600 V, 30 A GaN devices. The specific requirements of the power supply are listed in Table I. There are two isolated outputs in order to support both the switches of the phase leg. The inter-winding capacitance is required to be as small as possible, ideally lower than 5 pF. The switching frequency is limited to 1 MHz due to the gate driver high-temperature integrated chip used for this converter.

The active-clamp flyback is a better choice in this application, compared with the classic flyback and the LLC converter. Fig. 1 shows the simplified circuit model of the

TABLE I. GATE DRIVE POWER SUPPLY DESIGN REQUIREMENTS

Parameter	Value
Input Voltage	15 (±1 V) V
Output Voltage	6 V (2 %), 2 channels
Switching frequency	1 MHz
Primary/Secondary Insulation	> 2.5 kV (1 min @50 Hz)
Inter-windings Capacitance	< 5 pF
Operating Temperature	[-55°C; +200°C]
EMC requirement	DO160/MILSTD-461

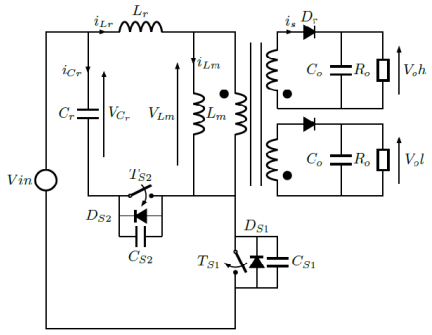

Fig. 1. Topology: active-clamp flyback

active clamp flyback converter. This topology adds an active-clamp snubber in the conventional flyback converter, composed of an auxiliary switch T_{S2} and a clamp capacitor C_r. With the active-clamp circuit, the energy stored in the leakage inductance can be used for both outputs and the two switches T_{S1} and T_{S2} can achieve soft switching, contributing a high efficiency. With the PCB-embedded transformer, the leakage inductance can represent 30% ~ 50% in the total primary inductance. Due to this large leakage inductance, the main switch in the classic flyback would experience very large turn-off voltage spike. In simulation with same devices, the active clamp flyback can achieve 88% efficiency, 19% higher than that of the classic flyback. In the other words, the active-clamp circuit offers the advantage of minimizing the power stored in the transformer. That allows the use of a smaller transformer compared to the classic flyback converter with comparable characteristics.

Compared with LLC converters, the selected topology is still a better candidate. It contains fewer transformer windings - three windings for two outputs. The LLC converter needs five windings and two more output diodes, which increase the transformer size significantly, and make it difficult to embed into PCB. On the other hand, the LLC brings higher efficiency (as high as 90%), but it is a small benefit compared with 88% efficiency based on the active clamp flyback.

As such, active clamp flyback topology was selected. In the following, two transformer designs are evaluated to assess their performance in this topology.

III. Coplanar-Windings Transformer Design

A. Transformer design

This design is based on a commercially available ferrite core, (Ferroxcube ER-9.5), with the central leg of th E core machined to form a U, as shown in Fig. 2b. The main target is to reduce the inter-windings capacitance drastically, so primary and secondary windings are jept separated, as visible in Fig. 2a. This structure has the advantage to not superimpose the primary and the secondary windings. The common area between primary and secondary is resume to the PCB copper thickness. The transformer design is based on the dead-time optimization for GaN transistors phase-legs, as explained below.

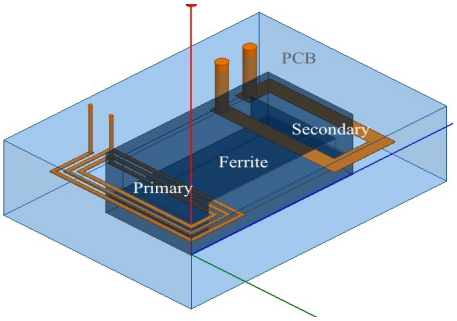

(a)

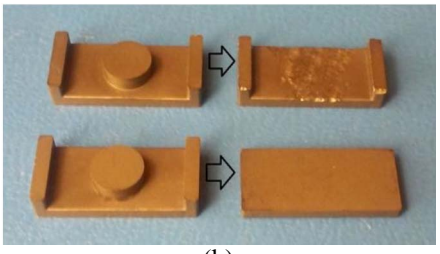

(b)

Fig. 2. (a) Coplanar-windings transformer design; (b) Machine U-I shape ferrites.

B. Design Method

During the dead time a current circulates between drain and source to charge and discharge the GaN parasitic capacitance. The equations are as follows and

$$L_m = \frac{\frac{V_{in}}{f^2}D^2 - 2L_r\left(\frac{P}{V_{in}f} + i_{Lr}(t_0)\frac{D}{f}\right)}{2\left(2L_r\left(\frac{P}{V_{in}f} + i_{Lr}(t_0)\frac{D}{f}\right)\right)} \quad (1)$$

$$\left|i_{Lr}(t_0)\right| \geq 2C_{S1/2}\frac{V_{in} + \frac{V_o}{n}}{t_{DT}} \quad (2)$$

$$n = \frac{V_o(1-D)}{DV_{in}}\frac{L_m + L_r}{L_m} \quad (3)$$

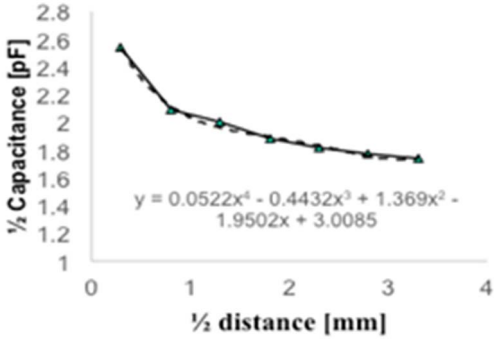

Fig. 3. Simulation (dash) and experimental measurements (solid) of the inter-capacitance for coplanar windings transformer design

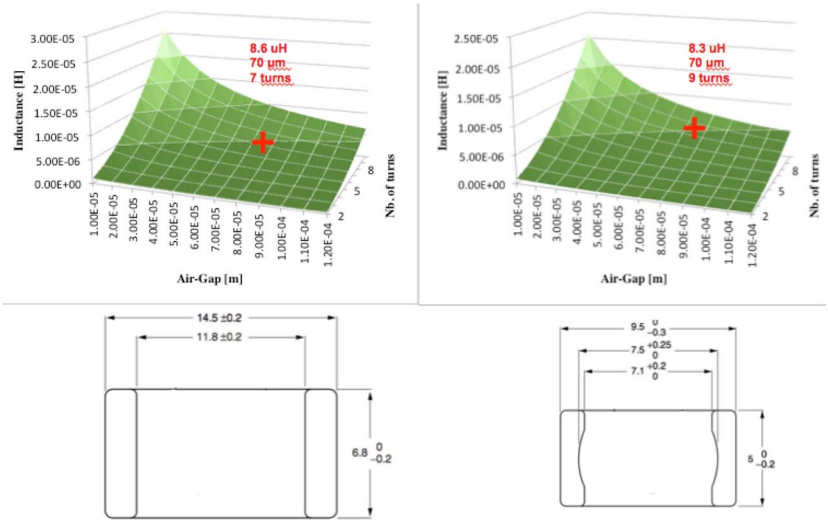

Fig. 4. Comparative transformer design 3D curve between ER 14.5 and ER 9.5 ferrite.

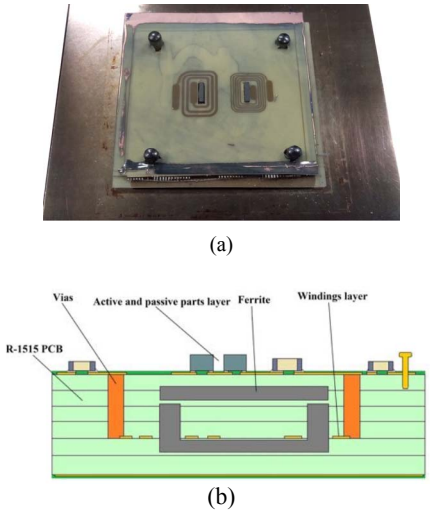

(a)

(b)

Fig. 5. (a) picture of the PCB stack before lamination [8]; (b) Schematic of power supply with coplanar windings PCB-embedded transformer.

summarize the elements to calculate the primary magnetizing inductance L_m. V_{in} is the input voltage, V_o is the output voltage, D is the duty cycle, f is the switching frequency, L_r is the leakage inductance of the transformer, P is the output power, $C_{S1/2}$ is the total capacitance of the switch junction capacitors, n is turn number ratio, and t_{DT} is the dead time between the two switches. In a high frequency soft-switching half-bridge, the dead-time control is a key point to reduce parasitic oscillations on the drain-source voltage responsible for EMI and switching losses. In a GaN HEMT half-bridge, it is not necessary to use external diode due to the 'body-diode' available in the HEMT structure. Nevertheless, this 'body diode' has an important voltage drop (2~3.1 V) which leads to conduction losses because of the resonant current. That is why a solution, experimentally verified, to set precisely the dead-time duration is proposed for a diode-less GaN half-bridge [7]. During dead-times, there is a capacitive transition in the half-bridge, where the current is flowing through the drain-source intrinsinc capacitor. There is a relation between the magnetizing inductance and the required current to charge and discharge the drain-source capacitors. Indeed by a proper choice of the dead-time in (2) and the current at switching in (1), the transistor losses can be more reduced even further. In Fig. 3, by using the Q3D software, the distance between the primary and the secondary windings (in order to reduce the isolation capacitance as low as possible) was optimized. This curve has to be balance by the width of each winding that means more or less copper losses.

A comparison was between two different ferrite sizes. This study allowed us to check if any improvement can be made on the volume but also for the losses. Two transformers were made, one transformer design with ER14.5 core, and one with an ER9.5 core. In Fig. 4 two 3D curve graphics show the chosen design point between volumes, primary inductance given in (2) and air-gap. The corresponding losses (copper and core) calculated for both designs using the Maxwell for two Ferroxcube magnetic materials with high Curie temperature point: 3C92 and 3F45. The high Curie temperature point is a requirement, as the final converter should be able to operate at 200°C.

Based on Fig. 4 and Table II the following conclusions can be drawn: first the efficiency of the converter is barely affected by the transformer loss with respectively 8 and 11% for ER14.5 and ER9.5 core of the total converter efficiency. In another hand the volume is dividing by two when we are using a smaller core. Therefore, the density of the converter will be higher with the ER9.5 core with a small increase of the loss. For the material 3C92 is not a high frequency material and the losses are higher than with 3F45 for a 1 MHz switching frequency.

In this practical case, the transistor used has an equivalent

TABLE II. LOSS COMPARATIVE RESULTS FOR 3F45 AND 3C92 MATERIALS.

	ER14.5	**ER9.5**
Volume/ cm^3	0.614	0.265
3C92 Total Losses (Copper+Core) /mW	65 +71	71+102
3F45 Total Losses (Copper+Core) /mW	65 +182	71+295

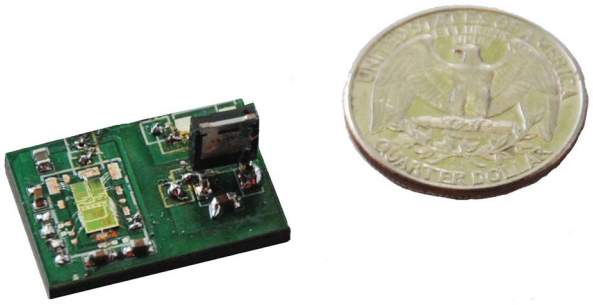

Fig. 6. First prototype with top components of the coplanar windings transformer.

drain-source capacitor of 50 pF for 30 V drain voltage. The current, in (1), has to be more than 102.6 mA if the dead-time value is 110 ns. In these conditions the magnetizing inductance in (2) has to be less than 5.4 μH. The transformer ratio is designed by the equation (3).

C. Experimental results

Fig. 5b shows a cross-section view of the PCB embedded transformer with different layers. In Fig. 5a the ferrite core and coplanar winding were embedded into the PCB (Panasonic R-1515W) to implement the transformer. All other components including active transistor devices were mounted on the top surface of the PCB substrate. The volume of this fabricated converter is 23 mm x 18 mm x 2.8 mm with an inter-capacitance measured of 0.77 pF, shown in Fig. 6. The global efficiency of the converter is about 74 % at 25°C. The losses are mainly affected by the voltage drop in the output rectifiers.

IV. Toroidal PCB-Embedded Transformer Design

A. Transformer design

A different design, named toroidal PCB-embedded transformer, is proposed, shown in Fig. 7. The toroidal core is placed in x-y plane and three copper windings – one primary and two secondary - wrap the core. The planar copper on the top and bottom sides layouts as PCB traces. The z-direction copper winding connection can be realized by via-holes or copper pins.

There is only one air gap cut in the core, to keep the core as one piece, which makes the structure stronger during lamination process and reduces the magnetic flux leakage. If two or more air gaps are distributed on the core, the air gap cannot be precisely controlled to be the desired value due to the high pressure in the lamination process. Besides, the core is hard to be in the same x-y plane if it is cut into several pieces. As for the air gap position, it locates out of windings to avoid extra AC winding loss, and between the two secondary windings to keep two secondary windings symmetric. Core material is selected as P61 from ACME. It has relatively low power loss coefficient compared with other products [10].

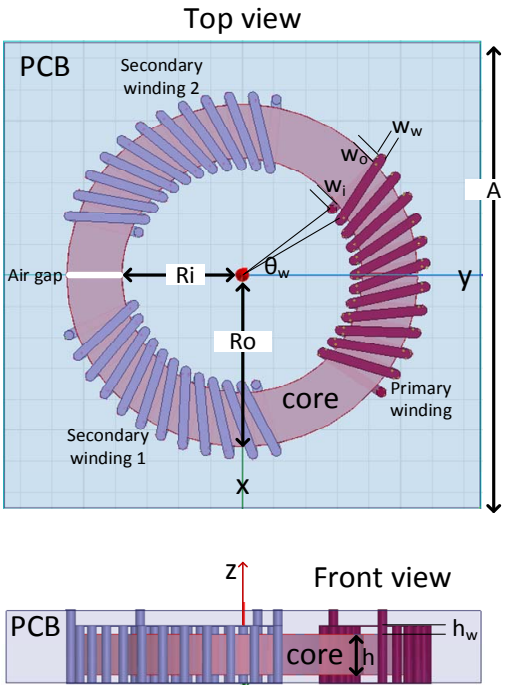

Fig. 7. Toroidal PCB-embedded transformer design.

TABLE III. Dimensions of the Toroidal PCB-Embedded Transformer Design

	Transformer Description	Optimized Value
R_i/mm	Core inner radius	3.7
R_o/mm	Core outer radius	5.65
h/mm	Core thickness	1.8
l_g/mm	Air gap width	0.1
w_w/mm	Turn width	0.2
w_i/mm	Space between winding and core at inner circle	0.5
w_o/mm	Space between winding and core at outer circle	0.5
h_w/mm	Space between winding and core in the vertical direction	0.1
Θ_w/degree	Angle between turns	2.86
t_w/mm	Winding copper thickness	0.0343
N	Turn number	10

B. Design method

An optimization is performed to have a smaller transformer volume, a smaller inter-capacitance and a smaller loss in this design, by optimizing the transformer dimension parameters in Fig. 7, listed in Table III. In order to do the optimization, first the boundary of the optimization input is clarified. To limited core size and to have an enough top circuit area, R_o should be smaller than 6 mm and larger than 4 mm. w_i, w_o, and h_w are required to be larger than 0.5 mm, 0.5 mm and 0.1 mm due the limited PCB manufacture ability. t_w has two options: 1 oz (0.0343 mm) or 2 oz (0.0686 mm). In order to achieve soft-switching, according to (1), (2), (3), the leakage inductance and magnetizing inductance has a limitation, with one more fact that leakage inductance takes 30% ~ 40% of the total primary inductance, found in the finished transformer samples. The outputs of the optimization are transformer volume, the total loss and the inter-capacitance.

Then the equations between the inputs and outputs are built. First the volume, it is can be calculated as follows taking a square surface on the top layer:

$$V = (2(R_o + w_o + ww))^2 (2h_w + h) \quad . \tag{4}$$

The loss can be separated into the core loss and the winding loss. The core loss can be calculated based on the estimated average magnetic field and the power loss coefficient P_v at 1 MHz provided by the magnetic manufacture as follows:

$$P_v = 10^{(2.8299 \times \log_{10}(\Delta B) - 2.2548)} \tag{5}$$

$$P_{core} = \pi P_v h (R_o^2 - R_i^2) \tag{6}$$

$$R_{DC} = 2N\rho_{copper}\frac{(R_o - R_i + w_i + w_o + 2ww + h + 2h_w)}{w_w t_w} \quad (7)$$

$$P_{winding} = (i_{rms-pri}{}^2 + 2i_{rms-sec}{}^2)(R_{DC} + R_{AC}) \ . \quad (8)$$

$i_{rms\text{-}pri}$ and $i_{rms\text{-}sec}$ are calculated primary and secondary current under different magnetizing inductance. The equivalent winding AC loss R_{AC} is estimated to a closed value from the FEA transient simulation. The loss model with the equations matches the FEA simulation within 10% error. The FEA simulation has 5% percent error from the experimentally transformer.

The inter-capacitance model is relatively complex to build compared with the loss model. There are two parts in the inter-capacitance calculation. One is total impedance of the equivalent capacitance from winding to core, in series with the resistance from primary side to secondary side on the core, and with the capacitance from core to the winding. This can be described with some analytical equations. The other part is the capacitance between the two windings without core, which is descripted with curve-fitting method based on the Q3D simulation results. However the error between the Q3D simulation and final measurements can be up to 35% due to the measurement accuracy, which reduces accuracy of the whole optimization.

There are two transformer samples with 1.3 mm and 1.8 mm thickness to verify the loss model and three samples with different inter-winding-angle to verify the inter-capacitance model.

Using the optimization software CADES, and the built models, the optimization process runs with two steps to draw a 3D Pareto surface – volume, loss, and inter-winding capacitance. In the first step, one optimization runs with fixed volume number and inter-winding capacitance value to get the smallest loss, by optimizing inputs. In special conditions, there is no solution to solve a fixed volume with a fixed inter-capacitance, and therefore it will give none under this condition. Once the solutions can output, the optimization runs within the solutions to find the smallest loss. The second step is to sweep the volume value and the inter-capacitance value

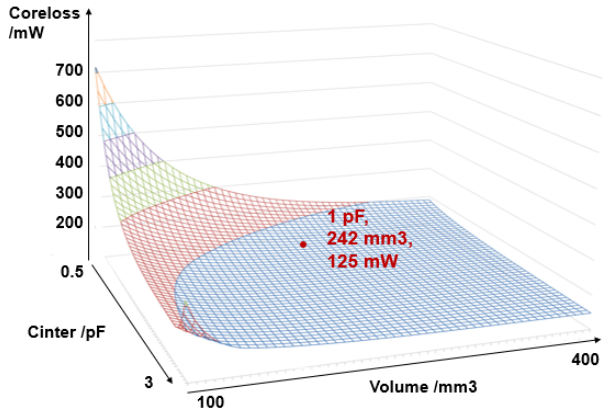

Fig. 8. Pareto surface within loss, inter-capacitance, and volume for the toroidal transformer design.

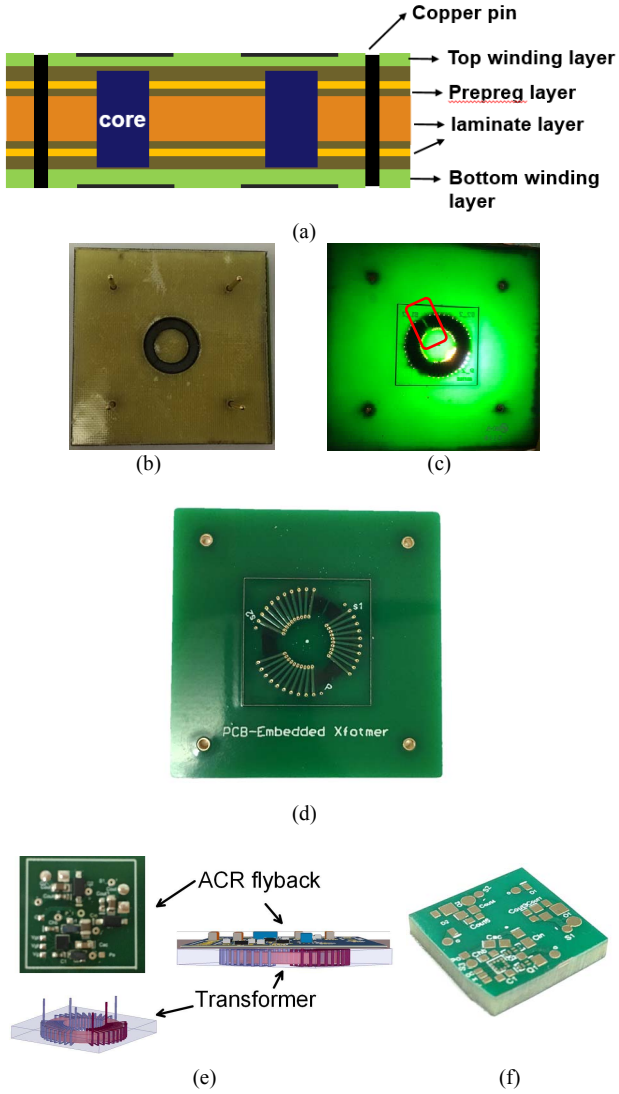

Fig. 9. (a) PCB lamination layer stack illustration; (b) layer stack before lamination; (c) toroidal PCB-embedded transformer, whose core and air gap are highlighted; (d) toroidal PCB embedded transformer; (e) connection of the toroidal PCB-embedded transformer and the converter; (f) converter after final lamination.

to have the 3D Pareto surface in Fig. 8. Each point on this surface is an optimized result. One points is selected according to the requirement as 242 mW loss, 1 pF inter-capacitance and 242 mm^3 volume. The corresponding dimensions are listed in Table III.

C. Lamination and experimental results

The PCB material layer stack before the lamination process is shown in Fig. 9a and Fig. 9b, where the toroidal core is place in the center of four copper pins. The copper pins are used to fix the layer position during press process in case the core center misses alignment with the winding center. Fig. 9c and Fig. 9d exhibit the toroidal PCB-embedded transformer after the press cycle, where the core, its air gap, and winding via-holes are displayed. It is also seen in this figure that the core and the three windings are accurately aligned. The

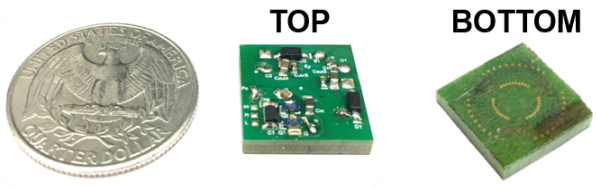

Fig. 10. ACR flyback with the toroidal PCB-embedded transformer

finished thickness of the transformer PCB is 2 mm. The measured inter-winding capacitance of the transformer is 1.6 pF, the primary magnetizing inductance is 3.5 μH and the leakage inductance is 1.7 μH.

In order to connect the transformer with the ACR flyback converter, the second lamination is processed as Fig. 9e shows, whose result is depicted in Fig. 9f. There are six via-holes to drill at the top converter layer, located at the exact winding input and output via-holes. The bottom of the transformer is also attached to a thin PCB layer to increase the transformer stability and isolation voltage. The final converter is illustrated in Fig. 10. The efficiency of the whole prototype is 85%, the volume 405 mm^3 (13 mm x 13mm x 2.4mm), and the power density 72.6 W/in^3.

V. Comparison Between The Two Designs

Table IV compares the three key characteristics of the two designs – coplanar and toroidal PCB-embedded transformer. The toroidal transformer core has a small size, compared with coplanar one. Therefore its total converter size is smaller, but with a larger inter-windings capacitance. The latter is mainly dominated by the distance between windings. If the core is larger, the primary and secondary can be placed with further distance, and as a result, the inter-winding capacitance is smaller. As for the converter efficiency, the toroidal design wins on the transformer loss, thanks to the core material with smaller loss coefficient to have less core loss. The toroidal design has 10 turns for each winding, and therefore a larger magnetizing inductance, then smaller current in the transformer and switches, which leads to smaller AC winding loss and smaller switch conducting loss.

For the high temperature consideration, first the curie temperature of the both cores is higher than 280℃. The PCB material is selected to hold a maximum point at 300℃. The thermal cycling test was performed to verify the stability of the transformers structure after 1000 cycles (30 min at 200°C and 30 min at -55°C with a slop of 10°C/min). Moreover, the coplanar windings method is to pot the ferrite with a dedicated layer for the winding in order to making the transformer. The winding is connected to the top circuit by pin connection. As a comparison, in the toroidal design, the conductive via-holes as winding is wrapped around the core. The reliability of the assembly against temperature variation is reduced due to the large number of winding via-holes. More prepreg layers in the structure help to exhaust air in the via-holes and the air gaps and to enhance the thermal reliability.

TABLE IV. Comparison between Two Transformers

	Co-planar	Toroidal
Volume/ mm^3	1159	405
Inter-capacitance/pF	0.77	1.6
Converter efficiency	74%	85%

Besides, the open structure with the external windings in the toroidal design may generate a significant magnetic field emission, which may not fit with the aeronautical standard. In order to reduce the emission generation, one shielding layer can be placed between circuit layer and transformer, and one more shielding layer is added at the bottom layer. With the extra shield layers, the volume of the transformer will increase 20%. From the point on the isolated voltage, the two secondary winding in the coplanar are quite close, resulting in a smaller isolation voltage.

Compared with the state of the art, the coplanar transformer has much smaller inter-winding capacitance. As a comparison, for commercial products with close volume, have a capacitance of 2.1 pF between primary and secondary [15]. The toroidal design wins on the efficiency compared with 70%~75% efficiency in the commercial products [15]. Both designs have two isolated outputs, contributing to a larger equivalent power density compared with the similar products with single output.

VI. Sumarry and Conclusions

In the paper, the magnetic PCB-embedded technique is introduced to build a high-integration high-efficiency and low inter-capacitance converter. The coplanar transformer embeds the modified ER core into PCB and achieves a very small inter-winding capacitance as 0.77 pF. The toroidal approach introduces the use of a toroidal-shape core inside PCB, and build a 3D Pareto surface based on an optimization, which brings a high efficiency of 85% at 2 W output, and a very small volume and small inter-winding capacitance.

References

[1] S. Yipeng, Z. Wenli, L. Qiang, F. C. Lee, and M. Mingkai, "High frequency integrated Point of Load (POL) module with PCB embedded inductor substrate," in *Energy Conversion Congress and Exposition (ECCE), 2013 IEEE*, 2013, pp. 1243-1250.

[2] C. M. Arturi and A. Gandelli, "High frequency models of PCB-based transformers," in *Circuits and Systems, 2001. MWSCAS 2001. Proceedings of the 44th IEEE 2001 Midwest Symposium on*, 2001, pp. 797-801 vol.2.

[3] Y. Su, Q. Li, and F. Lee, "Design and evaluation of a high-frequency ltcc inductor substrate for a three-dimensional integrated dc-dc converter," *Power Electronics, IEEE Transactions on*, vol. 28, no. 9, pp. 4354–4364, Sept 2013.

[4] P. Artillan, M. Brunet, D. Bourrier, J.-P. Laur, N. Mauran, L. Bary, M. Dilhan, B. Estibals, C. Alonso, and J. Sanchez, "Integrated lc filter on silicon for dc-dc converter applications," *Power Electronics, IEEE Transactions on*, vol. 26, no. 8, pp. 2319–2325, Aug 2011.

[5] Clyde F. Coombs, Jr., The Printed Circuits Handbook, McGraw-Hill, 6th Edition, 2008, Chapter 6.

[6] Inoue, O.; Matsutani, N.; Kugimiya, K., "Low loss MnZn-ferrites: frequency dependence of minimum power loss temperature," in *Magnetics, IEEE Transactions on* , vol.29, no.6, pp.3532-3534, Nov 1993

[7] R. Perrin; N. Quentin; B. Allard; C. Martin; M. Ali, "High Temperature GaN Active-Clamp Flyback Converter with Resonant Operation Mode," in *IEEE Journal of Emerging and Selected Topics in Power Electronics* , vol.PP, no.99, pp.1-1

[8] R. Perrin and al., "2 MHz High-Density Integrated Power Supply for Gate Driver in High-Temperature Applications" *2015 30th Annual IEEE Applied Power Electron. Conf. and Exp. (APEC*, 21-25 March. 2015.

[9] W. Yuan, X. Huang, P. Meng, G. Zhang and J. Zhang, "An improved winding loss analytical model of Flyback transformer," *Applied Power Electronics Conference and Exposition (APEC), 2010 Twenty-Fifth Annual IEEE*, Palm Springs, CA, 2010, pp. 433-438.

[10] X. Huang, J. Feng, W. Du, F. C. Lee and Q. Li, "Design consideration of MHz active clamp flyback converter with GaN devices for low power adapter application," *2016 IEEE Applied Power Electronics Conference and Exposition (APEC)*, Long Beach, CA, 2016, pp. 2334-2341.

[11] D. Hou, Y. Su, Q. Li and F. C. Lee, "Improving the efficiency and dynamics of 3D integrated POL," *2015 IEEE Applied Power Electronics Conference and Exposition (APEC)*, Charlotte, NC, 2015, pp. 140-145.

[12] W. Zhang, M. Mu, D. Hou, Y. Su, Q. Li and F. C. Lee, "Characterization of Low Temperature Sintered Ferrite Laminates for High Frequency Point-of-Load (POL) Converters," in *IEEE Transactions on Magnetics*, vol. 49, no. 11, pp. 5454-5463, Nov. 2013.

[13] W. Zhang, M. Mu, D. Hou, Y. Su, Q. Li and F. C. Lee, "Characterization of Low Temperature Sintered Ferrite Laminates for High Frequency Point-of-Load (POL) Converters," in *IEEE Transactions on Magnetics*, vol. 49, no. 11, pp. 5454-5463, Nov. 2013.

[14] D. Hou, F. C. Lee and Q. Li, "Magnetic characterization technique and materials comparison for very high frequency IVR," *2016 IEEE Applied Power Electronics Conference and Exposition (APEC)*, Long Beach, CA, 2016, pp. 657-662.

[15] Murata Power Solutions, 'NXE2 Series Isolated 2W Single Output SM DC/DC Converters', NXE2S1205MC datasheet.